Send Orders for Reprints to reprints@benthamscience.ae

The Open Cybernetics & Systemics Journal, 2015, *9*, 683-689

Open Access

Adaptive Sampling Rate Assignment for Block Compressed Sensing of Images Using Wavelet Transform

Luo Xin[1], Zhang Junguo[1,*], Chen Chen[2] and Lin Fantao[3]

[1]*School of Technology, Beijing Forestry University, Beijing 100083, China;* [2]*Department of Electrical Engineering, University of Texas at Dallas, Richardson 75080, USA;* [3]*China Electric Power Research Institute, Beijing, 100192, China*

Abstract: Compressed sensing theory breaks through the limit that two times the bandwidth of the signal sampling rate in Nyquist theorem, providing a guideline for new methods for image acquisition and compression. For still images, block compressed sensing (BCS) has been designed to reduce the size of sensing matrix and the complexity of sampling and reconstruction. However, BCS algorithm assigns the same sampling rate for all image blocks without considering the structures of the blocks. In this paper, we present an adaptive sampling rate assignment method for BCS of images using wavelet transform. Wavelet coefficients of an image can reflect the structure information. Therefore, adaptive sampling rates are calculated and assigned to image blocks based on their wavelet coefficients. Several standard test images are employed to evaluate the performance of the proposed algorithm. Experimental results demonstrate that the proposed algorithm provides superior performance on both the reconstructed image quality and the visual effect.

Keywords: Adaptive sampling rate assignment, block compressed sensing, still image, wavelet transform.

1. INTRODUCTION

With the rapid development of information technology, the demand for image information is growing. Meanwhile, how to store, process and transmit large amounts of image data has become a serious problem. Traditional still image compression standard [1, 2]: JPEG and JPEG2000 can remove image spatial redundancy and obtain a large compression ratio. However, there are some drawbacks: (1) Based on the Nyquist sampling theorem, the sampling rate can't be less than two times of the signal bandwidth. It may be difficult for a hardware system to meet a high sampling rate. (2) All the image transform coefficients are calculated, but only a few are retained. This leads to a waste of data computing and memory resources. (3) During data transmission, missing coefficients will affect the image reconstruction quality.

In 2006, E. Candes, D. Donoho and T. Tao proposed the Compressed Sensing (CS) theory [3-5]. Under certain conditions, a signal can be recovered from far fewer samples than required by the Nyquist sampling theorem. CS theory provides a breakthrough for image compression. However, for two-dimensional images, CS algorithm faces high computational complexity and large memory access. In order to solve these problems, Lu Gan proposed block-based compressed sensing (BCS) [6]. In BCS, an image is divided into blocks and sampling and reconstruction are conducted in a block-by-block manner. Therefore, the computational complexity of sampling and reconstruction are greatly reduced.

The BCS algorithm assigns the same sampling rate for all blocks within an image. However, due to piecewise smooth regions in an image, some image blocks may contain only a little information. For example, texture blocks contain more information (*e.g.*, edges) than smooth blocks. Blocks with little information can be reconstructed by fewer observations. Therefore, it is not necessary to assign the same sampling rate for all image blocks. The image structural information can be utilized, under the premise of total sampling rate unchanged, to adaptively allocate sampling rate for different image blocks.

Wavelet transform is an efficient image representation method that has been extensively used in image compression. It can capture the edge information in different scales and orientations. In our proposed adaptive sampling rate assignment method, wavelet transform coefficients of an image is used to analysis the structure information of each image block and adaptively allocate sampling rate for each block. The proposed adaptive sampling rate assignment method for BCS can improve the reconstruction performance significantly. The rest of this paper is organized as follows. Section 2 gives a brief review of CS and BCS. Section 3 describes the proposed adaptive CS algorithm of still images based on wavelet coefficients. Experimental results are given in Section 4. Finally, Section5 is the conclusion.

2. COMPRESSED SENSING

2.1. The Basic Principles of Compressed Sensing

Consider a real-valued signal $x \in R^N$, it is sparse with respect to a transform Φ. Then $x = \Psi\alpha$ and

1874-110X/15

$\|\alpha\|_0 = K << N$ (Where $\|\alpha\|_0$ represents the number of non-zero coefficient of vector α), the coefficient vector α can be reconstructed with high probability from its linear and non-relevant projections y.

$$y=\Phi x=A\alpha \tag{2-1}$$

Here, $y \in R^M$ is the vector of projections constituted by a small amount of linear, non-relevant measured values. $\Phi \in R^{M\times N}$ is a measurement matrix and $M = N$. $A \in R^{M\times N}$ is on behalf of $\Phi\Psi$, called sensing matrix. Under normal circumstances, $K<M = N$.

In essence, y can be regarded as a linear combination of all the columns of A corresponding $\alpha_i \neq 0$. Formula (2-1) actually implements a dimensionality reduction process, and can also be considered a data compression method. Compared to the dimensionality reduction process, we are more concerned about how to recover α from the coefficient vector y. That is solving the following equation:

$$\min_{\alpha}\|\alpha\|_0, \quad \text{s.t. } y=A\alpha \tag{2-2}$$

Since Eq. (2-1) is a group of underdetermined linear equations, solving (2-2) is NP-hard. But under the premise of α being sparse, if A satisfies the restricted isometry property (RIP) [5], then the problem can be solved by iterative greedy algorithms, such as OMP [7], StOMP [8] and CoSaMP [9]. After obtaining α, the original x can be reconstructed by $x=\Psi\alpha$.

2.2. Block Compressed Sensing

When CS is used to process image signal, the size of measurement matrix $\Phi \in R^{M\times N}$ will be very large, N typically is between 10^4 and 10^6, making the storage and computing very challenging. In order to solve this problem, Lu Gan proposed a compressed sensing method based on a block-based sampling strategy [6].

BCS procedure is described as follows. Consider an image with $N = I_r \times I_c$ pixels in total, the image is divided into small non-overlapping blocks with size of $B\times B$ each. Let x_m represent the vectorized signal of the m-th block, $m = 1, 2\cdots n, n = N / B^2$, then each block is sampled with the same measurement matrix Φ_B. The corresponding output CS vector y_m can be written as

$$y_m = \Phi_B x_m \tag{2-3}$$

where Φ_B is a matrix with size of $M_B \times B^2$, and $M_B = \lfloor subrate \times B^2 \rfloor, 0 \le subrate \le 1$. For the whole image, the equivalent sampling operator Φ in (2-1) is thus a block diagonal matrix taking the following form

$$\Phi = \begin{pmatrix} \Phi_B & 0 & \cdots & 0 \\ 0 & \Phi_B & & \vdots \\ \vdots & & \ddots & 0 \\ 0 & \cdots & 0 & \Phi_B \end{pmatrix}.$$

Compared with compressed sensing based on the whole image, BCS is faster; however, it poses serious blocking artifacts. To remove the blocking artifacts, BCS-SPL [10] introduces Wiener filtering into the image reconstruction process, and gradually improves the quality of reconstruction by iterative process. A BCS-SPL variant named MH-BCS-SPL was introduced in [11] to further improve the BCS-SPL using a post-processing procedure where multihypothesis prediction strategy was used. The multihypothesis prediction strategy was also employed for hyperspectral image reconstruction [12] and single-image super-resolution [13]. Given the computational efficiency and good reconstruction performance of BCS-SPL, this paper adopts the BCS-SPL as the CS reconstruction method and investigates the adaptive sampling rate assignment for the BCS-SPL.

3. ADAPTIVE COMPRESSED SENSING ALGORITHM

3.1. Overall Framework of Adaptive Compressed Sensing Method

Different from traditional imaging systems, CS belongs to the sampling process information, and each CS measurement contains global information of the image block. The amount of measurements contain useful information has a large impact on the reconstruction result. The original BCS algorithm assigns the same sampling rate for all image blocks. However, when an image is divided into small blocks, the different image blocks contain different amount of information. Blocks containing little information can be reconstructed by fewer observations than those containing more information. Thus it is possible to adaptively allocate different sampling rates for different blocks to improve the BCS-SPL reconstruction performance.

The framework of our proposed adaptive compressed sensing algorithm for images is presented in Fig. (**1**). It includes adaptive sampling rate assignment, CS sampling, quantization, coding and CS reconstruction. In this paper, we focus on the part of adaptive sampling assignment for different blocks.

3.2. Adaptive Sampling Rate Assignment using Wavelet Transform

Wavelet analysis is a time - frequency analysis method of signal. It has the characteristics of multiscale analysis. In both time and frequency domain, wavelet analysis has the ability to characterize local signal characteristics. It has a high frequency resolution and a low time resolution in the low frequency portion and a low frequency resolution and a high time resolution in the high frequency portion. It is particularly suitable for analyzing and detecting transient abnormality signal in the normal signal.

After wavelet transform, the transform coefficients of an image can be categorized into low frequency coefficients and

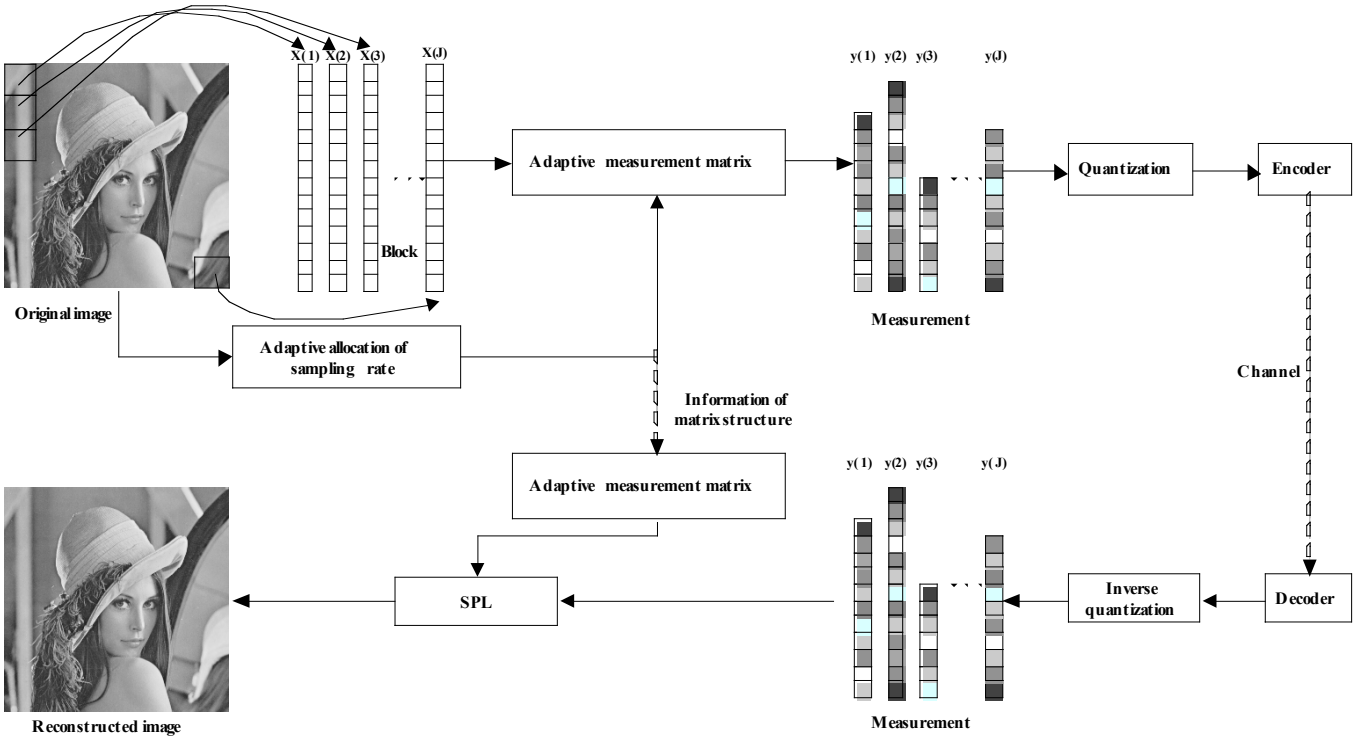

Fig. (1). Overall framework of the proposed adaptive compressed sensing method.

high frequency coefficients. In fact, the low frequency coefficients and high frequency coefficients are two different types of signals. Low-frequency coefficients epitomizes the image energy information, on the other hand, the high-frequency coefficients save rich detail information of an image. Therefore, we can observe and analyze an image by its wavelet coefficients, as shown in Fig. (**2**).

Fig. (2). The discrete stationary wavelet transform of the Lena image.

This paper presents an adaptive compressed sensing algorithm of still images based on wavelet coefficients. For easy operation, we use a discrete stationary wavelet transform (SWT). Therefore, our algorithm is named SWT-BCS-SPL. Compared with the conventional discrete wavelet transform (DWT), SWT has the "translation invariance" property [14]. The number of wavelet coefficients of the sub-band layers after decomposition is equal to the number of original image pixels, so we can apply the SWT on the whole image, then divide the image into blocks in the transform domain. Finally, we calculate the statistical results of absolute values of the vertical and diagonal high-frequency coefficients of each block. The sampling rate allocation is determined according to the absolute value of high-frequency coefficients of each block. The detailed process is shown in Fig. (**3**).

The value of the sampling rate SR is known, the size of block is $B \times B$, the number of image blocks is n. Thus, the total number of measurements can be obtained as $M = SR \times B^2 \times n$. In this paper, the sampling upper bound is denoted as $upper = 0.9 \times B^2$. In order to guarantee the basic quality of the reconstructed image, each block is assigned with the same fixed base sampling rate $FSR = W \times SR$, where W is a parameter that decides a fixed sampling rate. If W is larger, the fixed sampling rate for the blocks is higher, and $0 \le W \le 1$. According to the fixed sampling rate FSR, the fixed measurement number of each image block can be determined by $FM_i = \dfrac{FSR \times M}{n}$. After applying discrete stationary wavelet transform on the original image, the coefficient image are divided into blocks. The statistical results of absolute values of the high-frequency coefficients of each block, denoted as $coef(x_i)$, are calculated and the percentage of $coef(x_i)$ with respect to the whole image can be ob-

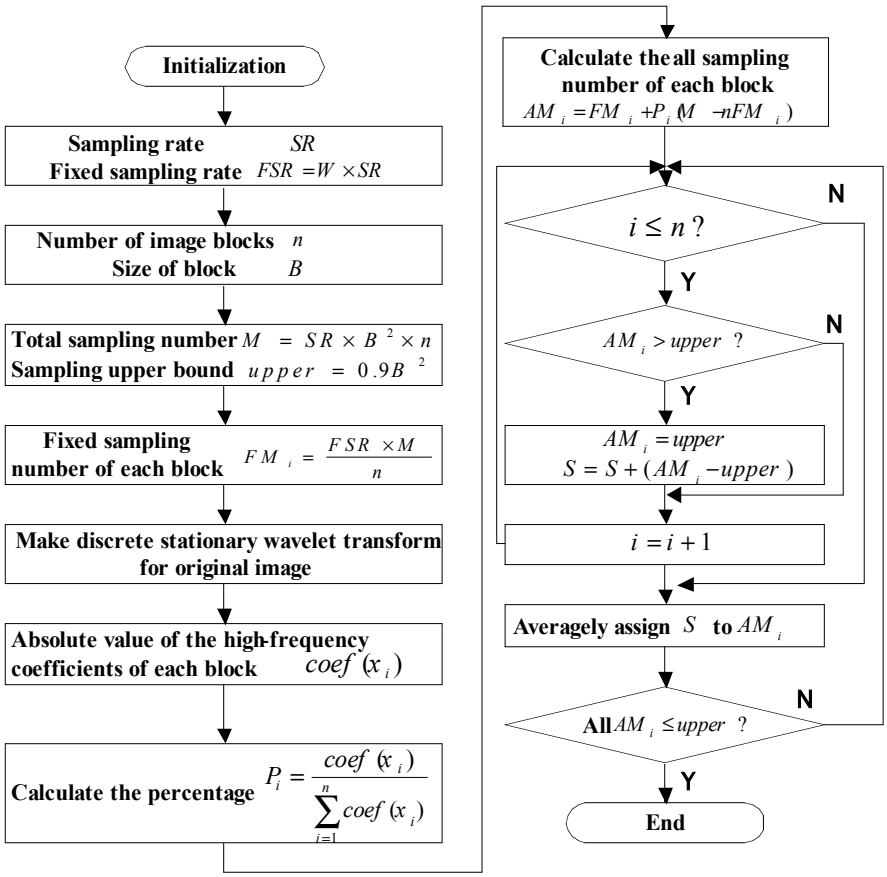

Fig. (3). Flow chart of the sampling rate assignment strategy based on wavelet coefficients.

tained by $P_i = \frac{coef(x_i)}{\sum_{i=1}^{n} coef(x_i)}$. We can then compute the total number of measurements for each block according to $AM_i = FM_i + P_i(M - nFM_i)$. If the total number of measurements for a block is larger than the upper bound, the excess measurements are accumulated for each block to obtain the total excess measurements for the whole image, $S = S + (AM_i - upper)$. The excess measurements are distributed equally to blocks that have $AM_i < upper$. This process may be repeated until all the blocks having sampling measurements are not out of the sampling upper bound. Here, the final number of measurements for each block is denoted as AM_i.

According to the sampling number of each block AM_i, the corresponding random measurement matrix is constructed and CS measurement is performed. Since the decoder needs to reconstruct the measurement matrix, the information of matrix structure needs to be transmitted. Compared with the original BCS, the adaptive compressed sensing algorithm needs to transmit the sampling number of each block to the decoder as well. Therefore, the bits cost will increase.

4. EXPERIMENTAL RESULTS

In this section, we evaluate the performance of the proposed adaptive compressed sensing algorithm based on wavelet coefficients (SWT-BCS-SPL), and compare it with the original BCS-SPL algorithm. For a more comprehensive evaluation of the reconstructed image quality, in addition to the commonly used PSNR, this paper uses structural similarity index measurement system (SSIM) [15] as an additional image quality evaluation criterion.

Six test images are used in our experiments including Lena, Barbara, Goldhill, Barbara2, Boat and Cameraman, as shown in Fig. (**4**). All the images have the size of 512×512 pixels. The experiments are conducted using MATLAB v7.8 (R2009a) on a PC with an Intel(R) Core(TM)2 Duo CPU T6670 at 2.19GHz and 2-GB of RAM. The sparse transform in BCS-SPL is the wavelet transform. It should be noted that all reconstruction quantity evaluations (PSNR and SSIM) are averaged over ten independent trials, since the performance of reconstruction varies due to the randomness of the sampling matrix.

4.1. Parameter Tuning

In order to analyze effect of the two main parameters in the adaptive sampling algorithm, block size B and the fixed sampling rate allocation parameter W, we select Lena image as the test image for the parameter tuning experiments.

Fig. (4). Test images in our experiments.

Table 1. The relation between the PSNR of the reconstructed image and the block size.

Algorithm	4×4	8×8	16×16	32×32
	PSNR	PSNR	PSNR	PSNR
SWT-BCS-SPL	38.15	38.73	38.48	38.26

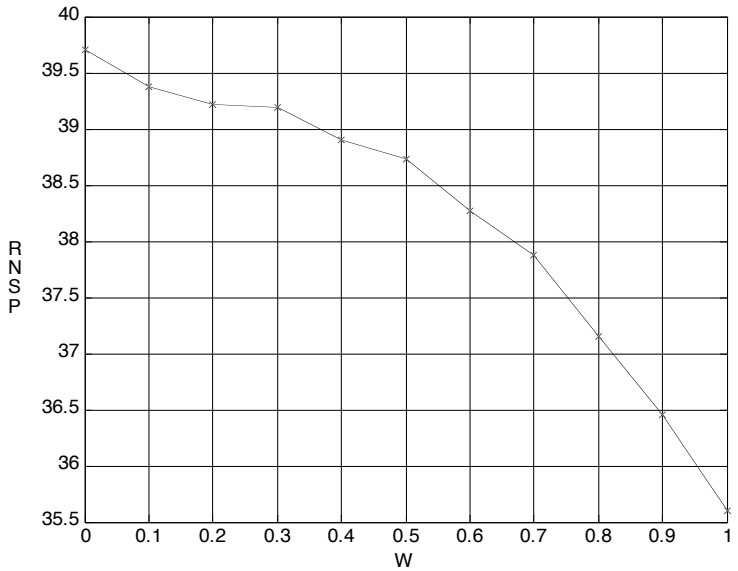

Fig. (5). The relation between PSNR of the reconstructed image and parameter *W*.

Under the experimental condition that the sampling rate is 0.5 and the fixed sampling rate allocation parameter W is 0.5, Table **1** shows the relation between the PSNR of the reconstructed image and the block size. It can be observed that when block size is 8 × 8, the image reconstructed by SWT-BCS-SPL algorithm achieved the highest PSNR value. Therefore, in our experiments, the block size B is set to 8 × 8.

Next, we analyze the parameter *W*. We set the sampling rate to 0.5 and block size B to 8×8, a set of *W* are tested. Fig. (**5**) shows the relation between the PSNR of the reconstructed

Table 2. Performance comparison between BCS-SPL and SWT-BCS-SPL at different sampling rates.

	Sampling Rate									
	0.1		0.2		0.3		0.4		0.5	
Algorithm	PSNR	SSIM	PSNR	SSIM	PSNR	SSIM	PSNR	SSIM	PSNR	SSIM
	Lena									
BCS-SPL	**26.37**	0.79	30.02	0.87	32.16	0.90	34.10	0.93	35.65	0.94
SWT-BCS-SPL	25.78	0.79	**31.29**	**0.88**	**34.29**	**0.91**	**36.83**	**0.94**	**38.73**	**0.95**
	Barbara									
BCS-SPL	**22.04**	**0.65**	23.65	0.74	24.77	0.80	26.15	0.85	27.51	0.89
SWT-BCS-SPL	20.90	0.63	**24.29**	**0.76**	**27.21**	**0.84**	**30.55**	**0.90**	**32.67**	**0.92**
	Goldhill									
BCS-SPL	**26.06**	**0.67**	28.49	0.77	30.07	0.83	31.47	0.87	32.73	0.90
SWT-BCS-SPL	23.69	0.66	**28.63**	**0.78**	**30.36**	**0.83**	**32.42**	**0.87**	**33.98**	**0.90**
	Barbara2									
BCS-SPL	**23.21**	0.63	25.29	0.76	26.94	0.83	28.67	0.88	30.26	0.91
SWT-BCS-SPL	22.86	**0.64**	**26.18**	**0.78**	**28.94**	**0.85**	**31.48**	**0.90**	**33.33**	**0.93**
	Boat									
BCS-SPL	**23.97**	0.66	27.11	0.77	29.07	0.83	30.81	0.87	32.25	0.90
SWT-BCS-SPL	23.76	**0.67**	**28.25**	**0.79**	**30.63**	**0.84**	**32.69**	**0.88**	**34.07**	0.90
	Cameraman									
BCS-SPL	24.08	0.81	28.01	0.90	30.60	0.94	33.11	0.96	34.89	0.97
SWT-BCS-SPL	**24.65**	**0.83**	**30.57**	**0.92**	**34.76**	**0.95**	**39.13**	**0.97**	**42.13**	**0.98**

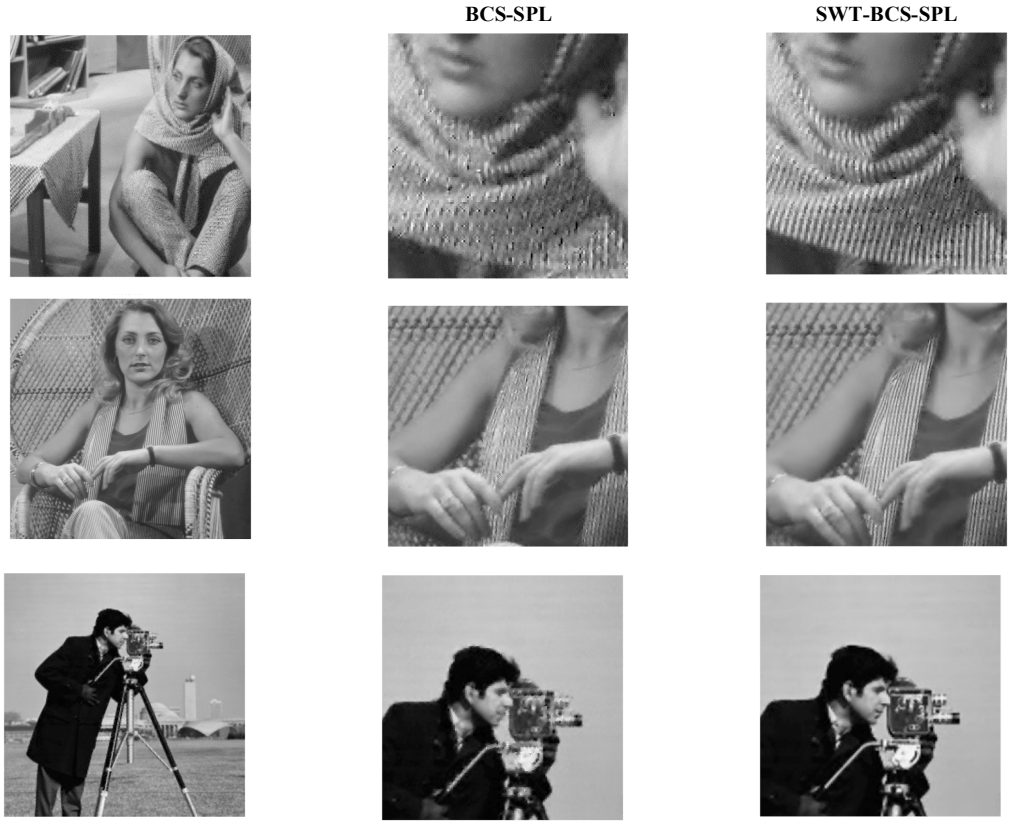

Fig. (6). Visual comparison of three reconstructed 512 × 512 images (shown in detail) for a sampling rate of SR = 0.3.

image and the fixed sampling rate allocation parameter W. It is obvious from the figure that, with the fixed sampling rate allocation parameter increases, the PSNR of the reconstructed image by SWT-BCS-SPL algorithm decreases. This also indicates that the adaptive sampling rate allocation can improve the quality of the reconstructed image. In this paper, the parameter W is set to an intermediate value of 0.5.

4.2. Comparison with BCS-SPL

The performance (PSNR and SSIM) of BCS-SPL and the proposed SWT-BCS-SPL at different sampling rates are listed in Table **2**. In the table, the best performance is emphasized by bold-faced font. It can be observed that SWT-BCS-SPL achieved improvements at almost all the sampling rates. These comparisons highlight the role of adaptive sensing. The results demonstrate that the proposed algorithm can improve the quality of the reconstructed image. The results show that the improvement of texture detail-rich images (*e.g.* Barbara and Barbara2) is more obvious. For Barbara image, the maximal PSNR gain reaches 5.16 dB and the average one is 2.3dB. For Barbara2 image, the maximal PSNR gain is 3.07 dB and the average one is 1.68dB. When the total sampling rate is rather low (*e.g.* SR=0.1) the advantage of SWT-BCS-SPL is not very clear or performs worse than BCS-SPL. The reason, we argue, is that since the total sampling number is very small, after adaptive allocation, the sampling number of each block is very similar, therefore, SWT-BCS-SPL is not effective.

To better illustrate the improvement, a visual comparison is provided in Fig. (**6**). From the figure, it can be seen that the details of three image recovered with SWT-BCS-SPL is more clear than BCS-SPL. It is because in SWT-BCS-SPL relatively high sampling rates are assigned to the edge and rich texture blocks and low sampling rates are assigned to the smooth blocks.

CONCLUSION

In this paper, an adaptive compressed sensing algorithm of still images based on wavelet coefficients was proposed to improve the reconstruction performance of the block-based compressed sensing (BCS). The algorithm utilized wavelet coefficients of each image block as a sampling rate allocation criteria to adaptively assign sampling rates for each block. High sampling rates were assigned to the blocks containing detailed information (*e.g.*, edges) and low sampling rates were assigned to the blocks containing less information (*e.g.*, smooth background). Compare with the original BCS with uniform sampling rate for all the block, the experimental results demonstrated a significant improvement in numerical and geometrical accuracy over the traditional block compressed sensing. However, since wavelet transform is complex, the computational complexity of the algorithm is increased. In our future work, a computationally efficient sampling rate assignment strategy will be investigated.

CONFLICT OF INTEREST

The authors confirm that this article content has no conflict of interest.

ACKNOWLEDGEMENTS

This work was funded by Beijing Higher Education Young Elite Teacher Project (Grant No.YETP0760), Fundamental Research Funds for the Central Universities (Grant No.TD2013-3) and Import Project under China State Forestry Administration (Grant No.2014-4-05).

REFERENCES

[1] G.K. Wallace, "The JPEG still picture compression standard", *Communications of the ACM*, vol. 34, pp. 30-44, 1991.

[2] D.S. Taubman, and M.W. Marcellin, "JPEG2000: Standard for interactive imaging", In: *Proceedings of the IEEE*, vol. 90, pp. 1336-1357, 2002.

[3] D. L. Donoho, "Compressed sensing", *IEEE Transactions on Information Theory*, vol. 52, pp. 1289-1306, 2006.

[4] E. J. Candès, "Compressive sampling", In: *Proceedings of the International Congress of Mathematicians*, Switzerland, 2006, pp. 1433-1452.

[5] E. J. Candès, J. Romberg and T Tao, "Robust uncertainty principles: Exact signal reconstruction from highly incomplete frequency information", *IEEE Transactions on Information Theory*, vol. 52, pp. 489-509, 2006.

[6] L. Gan, "Block compressed sensing of natural images", In: *Proceedings of the International Congress on Digital Signal Processing*, UK, 2007, pp. 403-406.

[7] J. A. Tropp, and A. C. Gilbert, "Signal recovery from random measurements *via* orthogonal matching pursuit", *IEEE Transactions on Information Theory*, vol. 53, pp. 4655-4666, 2007.

[8] D. L. Donoho, Y. Tsaig and J. L. Starck, "Sparse solution of underdetermined systems of linear equations by stagewise orthogonal matching pursuit", *IEEE Transactions on Information Theory*, vol. 58, pp. 1094-1121, 2012.

[9] D. Needell, and J.A. Tropp, "CoSaMP: Iterative signal recovery from incomplete and inaccurate samples", *Applied and Computational Harmonic Analysis*, vol. 26, pp. 301-321, 2009.

[10] S. Mun, and J. E. Fowler, "Block compressed sensing of images using directional transforms", In: *Proceedings of the International Congress on Image Processing,* Cairo, Egypt, 2009, pp. 3021-3024.

[11] C. Chen, E. W. Tramel, and J. E. Fowler, "Compressed-sensing recovery of images and video using multihypothesis predictions," In: *Proceedings of the 45th Asilomar Conference on Signals, Systems, and Computers*, Pacific Grove, CA, 2011, pp. 1193-1198.

[12] C. Chen, W. Li, E. W. Tramel, and J. E. Fowler, "Reconstruction of hyperspectral imagery from random projections using multihypothesis prediction," *IEEE Transactions on Geoscience and Remote Sensing*, vol. 52, pp. 365-374, 2014.

[13] C. Chen, and J. E. Fowler, "Single-Image Super-Resolution Using Multihypothesis Prediction," In: *Proceedings of the 46th Asilomar Conference on Signals, Systems, and Computers,* Pacific Grove, CA, pp. 608-612, 2012.

[14] G. Anbarjafari, S. Izadpanahi, and H. Demirel, "Video resolution enhancement by using discrete and stationary wavelet transforms with illumination compensation", *Signal, Image and Video Processing*, vol. 9, no. 1, pp. 1-6, 2012.

[15] Z. Wang, A. C. Bovik, and H. R. Sheikh, "Image quality assessment: from error visibility to structural similarity", *IEEE Transactions on Image Processing*, vol. 13, pp. 600-612, 2004.

Received: April 02, 2015 Revised: May 23, 2015 Accepted: June 06, 2015